Pergamon

Cement and Concrete Research 30 (2000) 1791–1799

CEMENT AND CONCRETE RESEARCH

# Hydration temperatures in large high-strength concrete columns incorporating slag

B. Sioulas[1], J.G. Sanjayan*

*Department of Civil Engineering, Monash University, Clayton, VIC 3800, Australia*

Received 17 November 1999; accepted 4 August 2000

**Abstract**

This paper presents the results of an investigation on the use of slag-blended cements in the production of high-strength concrete (HSC). The production of HSC requires high cement contents. Slag replacement can assist in reducing high hydration temperatures, which is a problem in concrete with high cement contents. This investigation studied the hydration temperatures of concretes with nominal strengths of 100, 80, 60 and 40 MPa. The improvements in hydration temperatures in the concretes were sought by replacing part of the ordinary Portland cement in the binder with slag. Slag replacement levels studied were of 70%, 50%, 30% and 0%. A ternary blend, containing Portland cement, slag and silica fume was also investigated in one of the columns. The study was based on square columns of size 800 × 800 mm in cross-section and 1200 mm high. Altogether, results of 11 columns are reported. The results indicate significant reductions in net temperature rise and thermal gradients can be achieved by the use of slag replacement in HSCs. 

*Keywords:* Hydration; Temperature; Granulated blast-furnace slag; Silica fume; High-performance concrete

## 1. Introduction

Advances in concrete technology over the last two decades have enabled the commercial production and supply of concretes with compressive strengths well in excess of 50 MPa. The acceptance of high-strength concrete (HSC) as a viable construction material has been driven by the numerous benefits it presents. HSC is often sought in the design of columns for high-rise buildings not only for its high compressive strength, but also for its increased stiffness [1]. Additionally, HSC provides a viable option when superior durability is required such as in the construction of offshore structures [2].

HSCs are characterized by a high binder content coupled with a low water to binder ratio. These features contribute to the high hydration temperatures inherent in HSC. In situ concrete temperatures in excess of 65°C have been reported [3–5]. The high temperatures can adversely affect the performance of the concrete. Detrimental effects associated with high temperatures include the risk of thermal cracking. Thermal cracking will occur when thermal stresses arising from the differential movement of the concrete upon cooling, exceed the tensile strength of the concrete. As a result of thermal cracking, high early temperatures can be responsible for loss of strength in concrete in the long term [6,7].

The problem is exacerbated when HSC is utilized in the construction of members with large cross-sectional dimensions [8]. The geometry of a member governs the magnitude of heat lost to the environment. Consequently, the temperature development profile experienced by the element is accordingly affected. This is pertinent in large HSC columns used in the lower stories of tall buildings.

In view of the factors outlined above, the favorable thermal characteristics [9] of slag-blended cements are often sought in the production of HSC. Slag is incorporated into the concrete mix with the aim of alleviating high early temperature development. Consequently, the risk of thermal cracking is mitigated as is the potential for regressed strength development in the long term.

This paper outlines the in situ thermal characteristics exhibited by large HSC columns incorporating slag-blended cements within the mix. The development of peak tempera-

* Corresponding author. Tel.: +61-3-9905-4985; fax: +61-3-9905-4944.

*E-mail address*: jay.sanjayan@eng.monash.edu.au (J.G. Sanjayan).

[1] Current address: Blue Circle Southern Cement Limited, Greystanes, NSW 2145, Australia.

0008-8846/00/$ – see front matter 
PII: S0008-8846(00)00387-2

Table 1
Mix proportions per cubic meter

| Mix type | 100GP | 100GB70/30 | 100GB50/50 | 100GB30/70 | 100GB45/45SF10 |
|---|---|---|---|---|---|
| Cement (kg) | 550 | 385 | 275 | 165 | 247.5 |
| Slag (kg) | 0 | 165 | 275 | 385 | 247.5 |
| Silica fume (kg) | 0 | 0 | 0 | 0 | 55 |
| Water (kg) | 165 | 165 | 165 | 165 | 165 |
| Coarse agg. (kg) | 1340 | 1330 | 1320 | 1320 | 1330 |
| Fine agg. (kg) | 520 | 510 | 510 | 510 | 510 |
| SP (kg) | 8.7 | 10.5 | 9.3 | 9.5 | 13.3 |
| W/B | 0.3 | 0.3 | 0.3 | 0.3 | 0.3 |
| Slump (mm) | 100 | 150 | 130 | 130 | 150 |

| Mix type | 80GP | 80GB50/50 | 60GP | 60GB50/50 | 40GP | 40GB50/50 |
|---|---|---|---|---|---|---|
| Cement (kg) | 500 | 250 | 400 | 200 | 360 | 180 |
| Slag (kg) | 0 | 250 | 0 | 200 | 0 | 180 |
| Water (kg) | 175 | 175 | 180 | 180 | 180 | 180 |
| Coarse agg. (kg) | 1260 | 1240 | 1310 | 1300 | 1130 | 1120 |
| Fine agg. (kg) | 610 | 600 | 630 | 630 | 830 | 820 |
| SP (kg) | 7.6 | 5 | 1.5 | 2.2 | – | – |
| W/B | 0.35 | 0.35 | 0.45 | 0.45 | 0.5 | 0.5 |
| Slump (mm) | 100 | 130 | 100 | 120 | 100 | 100 |

tures and temperature distributions across the cross-section of the columns is evaluated as are the thermal gradients encountered in each column.

## 2. Experimental outline

The objective of the ensuing experimental investigation was to assess the influence of slag replacement on the in situ temperature characteristics of the large concrete columns cast. The columns cast were 800 mm × 800 mm in cross-section and 1200 mm in height. The top and bottom surface of the columns were insulated using 50-mm-thick expanded polystyrene form to simulate an infinitely long column for temperature distribution purposes.

### 2.1. Concrete mixes and materials

Description of the labeling system adopted for the columns cast are as follows: *x*GP, where GP indicates General Purpose Portland cement and *x* indicates the strength grade; *x*GB*y*/*z*, where GB indicates General Blended cement, *x* indicates the strength grade and *y* and *z* indicate percentage of Portland cement and slag in the binder, respectively. 100GB45/45SF10 is a mix containing 45% Portland cement, 45% slag and 10% silica fume. At each strength grade, a mix incorporating 100% ordinary Portland Cement (Type GP) was produced to serve as a reference against which the slag blend mixes could be directly compared. The mix designs adopted for the investigation are shown in Table 1.

The coarse aggregate used in this investigation is basalt with a maximum size aggregate between 10 and 14 mm. The specific gravity and absorption of this aggregate are 2.95% and 1.2%, respectively. The fine aggregate was a sand from Lyndhurst with a fineness modulus of 2.2. The specific gravity and absorption of the fine aggregate are 2.65% and 0.5%, respectively.

The details of chemical and physical properties of other materials used in this investigation are provided in Table 2.

Table 2
Chemical and physical properties of materials used in this investigation

| Material | Chemical contents (w/w, %) | SG[a] | LOI[b] (%) | SSA[c] ($m^2$/kg) |
|---|---|---|---|---|
| Cement[d] | $C_3S$, 63; $C_2S$, 11; $C_3A$, 1.7; $C_4AF$, 17 | 3.15 | 1.2 | 350 |
| Slag[e] | $SiO_2$, 33.21; $Al_2O_3$, 12.58; $Fe_2O_3$, 0.22; MgO, 5.87; CaO, 39.29; $Na_2O$, 1.27; $TiO_2$, $K_2O$, 0.36; $SO_3$, 3.38 | 2.85 | 1.7 | 430 |
| Silica fume | $SiO_2 > 92$; $C < 6$; $Fe_2O_3 < 0.3$; $Si < 0.1$; $Al_2O_3 < 0.2$; $MgO < 0.2$; $CaO < 0.1$; $K_2O < 0.3$; $P_2O_5 < 0.2$ | 2.1 | 2.4 | 17,000–20,000 |
| Super-plasticizer | Naphthalene formaldehyde condensate type, 40% solids | 1.2 | – | – |

[a] Specific gravity.
[b] Loss of ignition.
[c] Specific surface area.
[d] Ordinary Portland cement.
[e] Ground granulated blast-furnace slag with 5% gypsum processing addition.

### 2.2. Formwork

The formwork used to cast the concrete was made from 3-mm mild steel plates welded to angle sections. It consisted of two full-length, 1200-mm-high side panels and six 400-mm-high segments. These smaller segments were individually bolted onto the full-length side panels to form the formwork as shown in Fig. 1.

### 2.3. Layout of thermocouples

A grid of thermocouples was used to monitor the cross-sectional temperature development profiles within each column. The grid was located 350 mm above the base of the columns. The geometric location of each thermocouple within the cross-section of the column is shown in Fig. 2. Thermocouples were located along three arms set at 90°, 60° and 45° from the side face of the column, and these have been denoted as Arm (90), Arm (60) and Arm (45), respectively. This layout was adopted to utilize the octagonal symmetry of the rectangular cross-section.

The arms, however, were not all placed within one octant so as to allow sufficiently large gaps for the concrete to be placed without hindrance and to reduce the risk of disturbing the thermocouples. On each of the three arms, thermocouples were installed at 0, 25, 50, 100, 200 and 400 mm from the side face of the columns. In all, 16 thermocouples were installed. The congestion of thermocouples near the surface of the column aimed to monitor the large thermal gradients anticipated there. Zinc-plated all-thread rod was used to support the thermocouples in position.

### 2.4. Temperature monitoring instrumentation

Type T copper/nickel thermocouples were used to conduct temperature monitoring. The thermocouples were prepared by being soldered at the hot junction and being covered with heat-shrink tubing to prevent the ingress of moisture. The cold junction of the thermocouple was connected to a terminal box with temperature sensors for cold junction compensation. Data was acquired using a DT100 datataker controlled by a laptop computer. Data was collected every 30 s and averaged over each 20 min time increment for a period of 72 h.

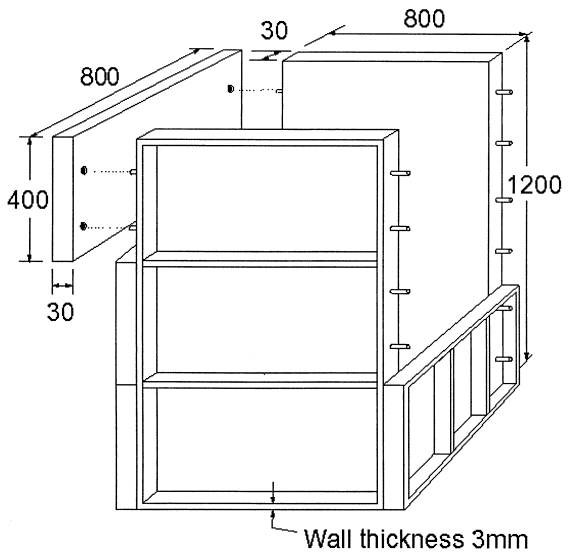


Fig. 1. Steel formwork.

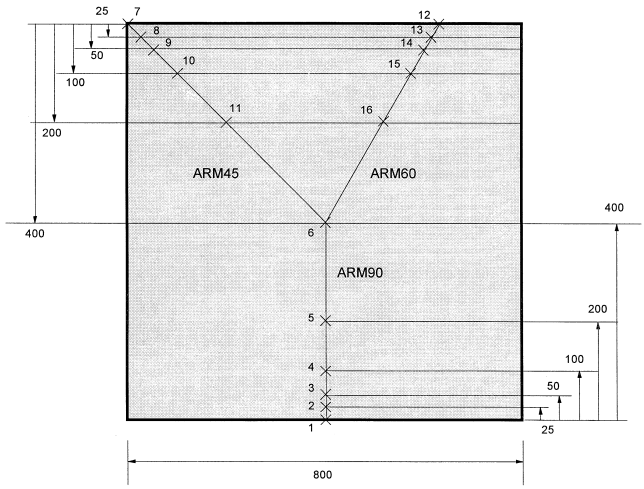


Fig. 2. Layout of thermocouples.

## 3. Temperatures at the centre of the columns

### 3.1. Temperature profiles

The temperature vs. time curves experienced at the center of all Grade 100 columns are shown in Fig. 3. Temperature curves for Grades 80, 60 and 40 columns are shown in Fig. 4. In these figures, *T*(C) indicates the temperature measured at the center of the columns, i.e., the thermocouple location 6 in Fig. 2.

The general shape of the GP curves is similar for all the strength grades investigated. An initial retardation period is exhibited followed by a rapid rise in temperature until a peak value is obtained. The peak temperature is sustained for a relatively short period of time, after which gradual cooling of the concrete commences. The retardation period is most prominent for the 80- and 100-MPa columns and is represented by a well-defined plateau on the curve immediately after casting, where negligible rises in temperature are recorded. The 80- and 100-MPa mixes experienced a retardation of approximately 2 and 5 h, respectively. The retardation period can be attributed to the high dosages of superplasticizer, which were incorporated into the mixes to produce a workable concrete. The plateau is non-existent in the 40- and 60-MPa column temperature profiles. This was expected as the 40-MPa mix did not require plasticizing while the 60-MPa concrete contained only a small dosage of superplasticizer.

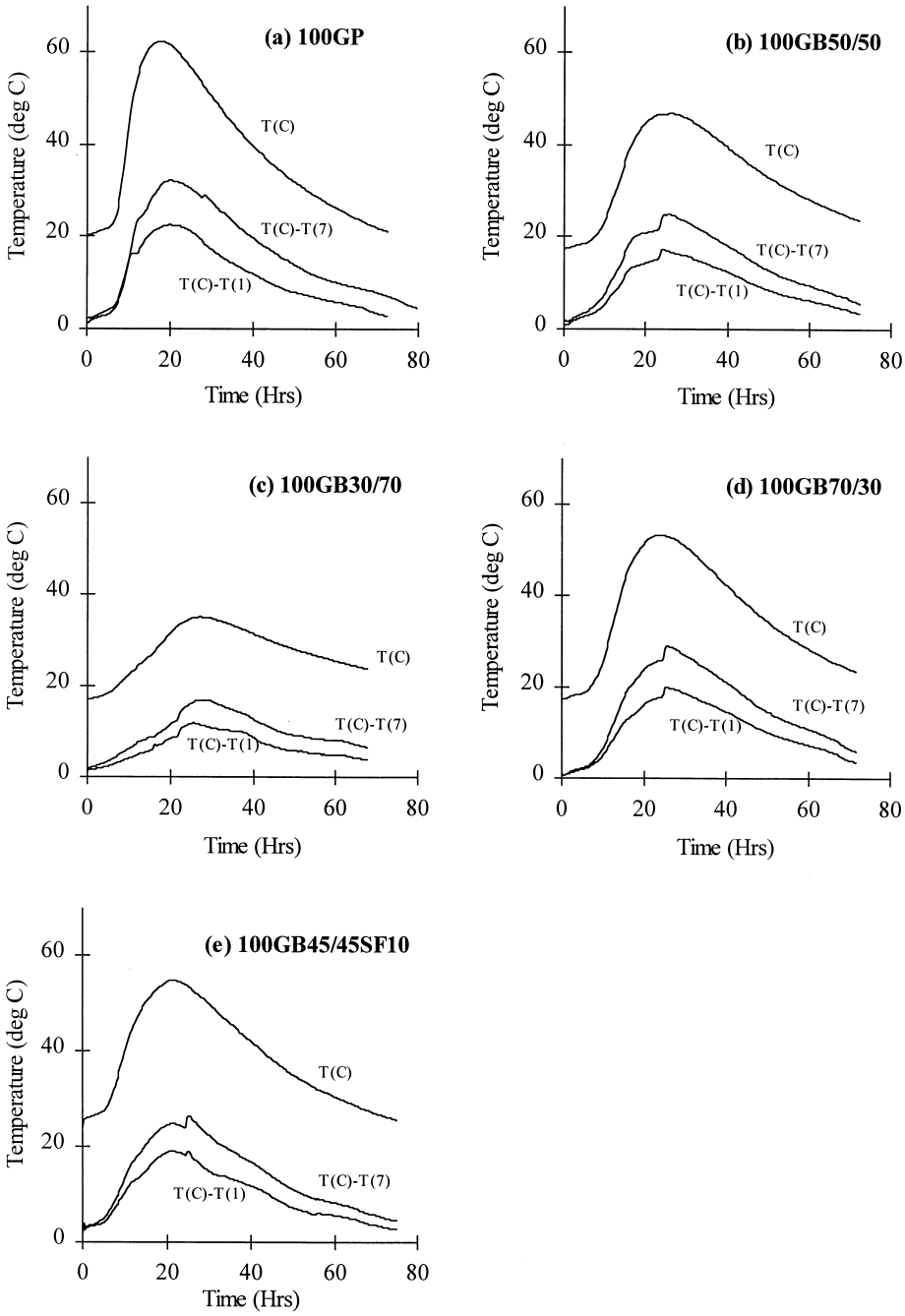


Fig. 3. Temperature curves for Grade 100.

The GB temperature development curves followed a similar trend at all strength levels, but varied noticeably in some aspects from the properties exhibited by their companion GP curves. Once again, the 80- and 100-MPa columns exhibited some initial hydration retardation, 5 and 7 h, respectively, while the 40- and 60-MPa profiles realized temperature rises immediately after casting. The rise in temperature experienced by the GB mixes was much more gradual than that realized by the GP columns; a more steady climb to peak temperature was recorded. This can be attributed to the latent hydraulic properties inherent in slag. The hydration of slag is a secondary reaction which proceeds after a sufficient quantity of calcium hydroxide crystals are available from the hydrating cement grains [10]. Accordingly, the slower hydration results in a more gradual development in temperature. Additionally, in contrast to the defined peaks exhibited by the GP profiles, the GB columns realized a flatter peak on the temperature profile as a result of sustaining peak temperature for a longer duration.

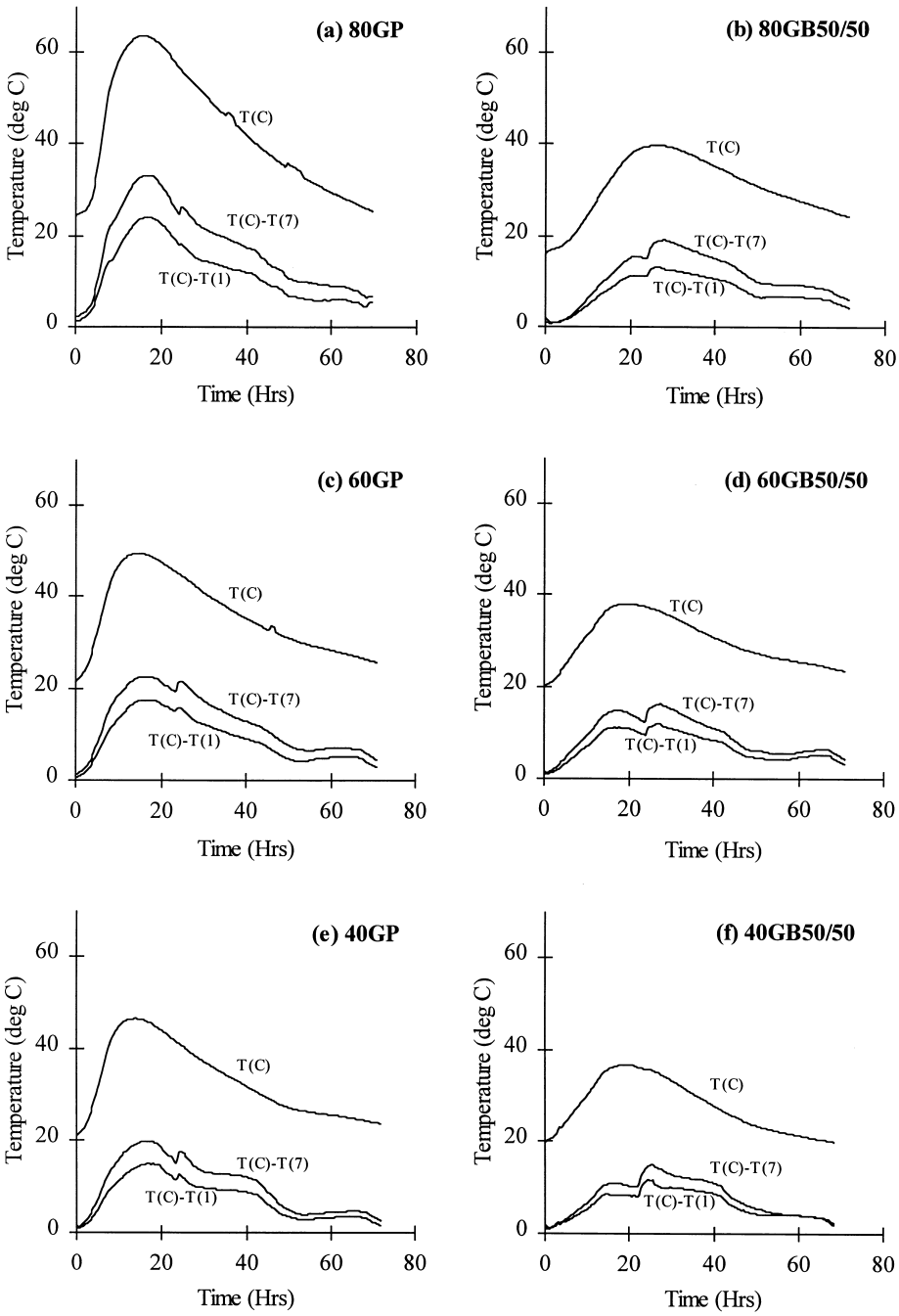


Fig. 4. Temperature curves for Grades 80, 60 and 40.

Finally, the cooling phase exhibited by the GB profiles was more gradual than that exhibited by their companion profiles at the 80- and 100-MPa grades. The cooling legs of the 40- and 60-MPa columns were virtually identical for both the GP and GB concretes. Cooling of the concrete commences when the quantity of heat dissipated to the environment exceeds the amount of heat generated within the element. The cooling phase of a hydrating concrete is generally regarded as the critical phase governing the occurrence of thermal cracking [11,12]. The slower cooling rates exhibited by the slag blends may assist in reducing the stresses generated and thus alleviating the tendency for cracking.

### 3.2. Peak and net temperature rise

The rise in in situ temperature at the center of the columns, above the initial concrete temperature, increased with increasing concrete strength grade for both the GP and GB columns (Table 3).

Table 3
Maximum peak and net temperature rises

| Column designation | Initial concrete temperature (°C) | Occurrence of peak temperature | | Maximum net temperature rise (°C) |
|---|---|---|---|---|
| | | Temperature (°C) | Time after casting (h) | |
| 40GP | 20 | 46.5 | 13.67 | 26.5 |
| 40GB50/50 | 18 | 36.5 | 18.0 | 18.5 |
| 60GP | 20 | 49.5 | 14.0 | 29.5 |
| 60GB50/50 | 19 | 38 | 18.67 | 19.0 |
| 80GP | 23 | 63.5 | 15.67 | 40.5 |
| 80GB50/50 | 15 | 40.0 | 26.0 | 25.0 |
| 100GP | 18.5 | 62.5 | 17.33 | 44.5 |
| 100GB70/30 | 17 | 53.5 | 23.33 | 36.5 |
| 100GB50/50 | 17 | 47.0 | 25.67 | 30.0 |
| 100GB30/70 | 17 | 35.0 | 27.0 | 18.0 |
| 100GB45/45SF10 | 21 | 54.9 | 21.33 | 34.0 |

Some researchers have reported [13,14] a reduction in net temperature rise at higher strength levels, attributable to the reduced amount of water available for hydration. No such reductions in have been observed in the results shown in Table 3. However, the peak temperature realized by the 80GP column, 63.5°C, was 1° higher than that observed in the 100GP column. This can be attributed to the fact that the initial concrete temperature was 6°C higher in the 80GP concrete due to higher ambient temperature during casting.

The net temperature rise encountered at the center of the columns was substantially reduced with the inclusion of slag into the binder at all the strength grades investigated. At the 40-, 60-, 80- and 100-MPa strength levels, 50% slag replacement resulted in an 8°C, 10.5°C, 15.5°C and 14.5°C drop in net temperature rise, respectively.

At the 100-MPa strength level where slag replacements of 30%, 50% and 70% were evaluated, a progressive reduction in maximum temperature rise was obtained with increasing slag percentages as shown in Table 3.

Progressive reduction in temperature with increasing slag content has also been encountered by other researchers. Mak and Lu [15] observed a 5%, 10% and 20% reduction in net temperature rise at 30%, 50% and 70% slag replacement, respectively, in comparison to a 100% Portland cement concrete at the 80-MPa strength level. Wainwright and Tolloczko's [16] data indicate net temperature reduction in temperature rise of approximately 10°C could be obtained with a 70% slag blend for Grade 25 and Grade 45 concretes. However, in contrast to the authors' results, Kokubu et al. [17] found that the adiabatic temperature rise increased at slag replacement levels of 35% and 55% while a significant reduction in temperature was encountered at 70% replacement.

The ternary blend incorporating 10% silica fume into the binder exhibited a net temperature rise of 34°C. Partial replacement of slag and cement in the 50% slag concrete with silica fume resulted in the triple blend moderately increasing the net temperature rise in comparison to the concrete containing 50% slag from 30°C to 34°C. Consequently, the incorporation of silica fume into the binder at the expense of the slag mitigated the reduction in temperature realized when slag was the only supplementary material present. However, the ternary blend recorded a lower net temperature rise in comparison to the GP column of approximately 10°C. This was also observed by Yurugi et al. [18] who also showed that in ternary mortars incorporating Portland cement, silica fume and slag, a significant reduction in temperature rise could be achieved when the slag content exceeded 40%.

### 3.3. Rate of temperature rise

The time required to achieve peak temperature was found to be related to the concrete strength grade (w/b ratio), as well as the binder composition. For all the columns investigated, the time required to reach peak temperature increased with increasing concrete strength grade, as shown in Table 3.

Increasing the strength grade from 40 to 100 MPa in the GP columns was accompanied by a progressive increase in the time needed to achieve peak temperature. The same trend was also exhibited by the slag blends.

The inclusion of slag into the concrete resulted in a delay in the time required to attain peak temperature irrespective of the grade of concrete under consideration. In comparison to the GP concrete, the concrete incorporating 50% slag into the binder required an additional 4.33, 5, 10.33 and 8.33 h to reach peak temperature at the 40-, 60-, 80- and 100-MPa strength grades, respectively. Results from the columns cast using the 100-MPa-strong concrete indicate that the time lag associated with developing peak temperature progressively increases with increasing slag content. The ternary blend incorporating silica fume developed its peak temperature 4 h prior to the 100GB50/50 column. The more rapid hydration of the silica fume being responsible for the greater rate of temperature rise.

In the case of the 80- and 100-MPa columns, the slag blends were developing peak temperatures 23–26 h after casting, which coincides with the formwork removal time of 24 h.

## 4. Cross-sectional temperature variations

Large differences in temperature between the center and surface of the column cross-section promote large thermal gradients which can potentially induce thermal cracking. If thermal cracks do develop, depending on their severity, they can diminish the integrity or serviceability of the concrete element and in severe cases can significantly reduce its durability. Additionally, in some instances it may be desirable to mitigate the potential for thermal cracking for architectural requirements.

### *4.1. Influence of formwork removal time*

Figs. 3 and 4 show the temperature–time histories at the center of the columns and the difference in temperature between the center and surface along the perpendicular, Arm (90), and diagonal, Arm (45), arms. $T$(C) refers to the thermocouple at the center of the column while $T$(1)and $T$(7) refer to the thermocouples located on the surface of the column on Arm (90) and Arm (45), respectively. The nomenclature $T$(C)–$T$(1) and $T$(C)–$T$(7) represent the absolute difference in temperature between the center and surface thermocouples. The curves provide valuable information concerning the influence of the timing of formwork removal.

Striking of the formwork took place 24 h after casting. An inspection of the curves representing the difference between surface and center temperatures reveals a well-defined, sharp rise in temperature coinciding with the removal of the formwork. The rise occurs because at the time of formwork removal, the column surface temperature had not yet reached ambient. Removal of the formwork exposes the column surface to the prevailing ambient conditions. Subsequently, rapid cooling of the surface proceeds as heat is dissipated to the environment in order to satisfy thermal equilibrium. On the other hand, the internal portion of the column is not sensitive to instantaneous fluctuations in ambient conditions and the temperature development profile in this region remains unaffected. Consequently, the sudden drop in surface temperature results in the difference in temperature between the center and surface rising, and this is recorded on the curve with a small but sudden change in temperature.

Formwork removal can therefore influence the magnitude of temperature variation between the internal and external region of an element. This is relevant as limiting values of temperature differences (e.g. 20°C) are often imposed with the intent of reducing thermal gradients and consequently mitigating the potential for thermal cracking.

It is evident from Figs. 3 and 4 that the GP columns attained maximum differential temperatures prior to formwork removal and the subsequent increase in differential upon removal of the formwork did not exceed the original value. In contrast to this, however, striking the forms at 24 h from the GB columns resulted in a temperature difference, which exceeded the previously recorded maximum. As mentioned earlier, in this instance, 3-mm mild steel was used as formwork for all the columns. Consequently, the magnitude of benefit derived from the use of slag in terms of alleviating temperature differentials, is sensitive to the timing of formwork removal. Delaying removal of the formwork to 72 h in this instance, would have yielded the maximum benefit of utilising slag.

It should be noted that the type of formwork used will have a bearing on the outcome of the temperature differences ascertained [13,19]. The heat circulation capacity of the formwork will influence its ability to dissipate heat to the environment and peak temperatures and temperature differentials will be affected accordingly.

Despite the increase in temperature differential realized by the slag-blended concrete upon formwork removal, the slag blends outperformed the GP columns with respect to minimizing temperature differentials, consistently recording lower differentials at all the strength grades investigated. Table 4 presents the maximum temperature differentials

Table 4
Maximum temperature differences between the center and surface of the columns

| | Occurrence of maximum temperature difference | | | | Occurrence of maximum temperature difference before formwork removal | | | |
|---|---|---|---|---|---|---|---|---|
| | Temperature difference (°C) | | Time (h) | | Temperature difference (°C) | | Time (h) | |
| Column designation | Arm (90) | Arm (45) | Arm (90) | Arm (45) | Arm (90) | Arm (45) | Arm (90) | Arm (45) |
| 40GP | 15.0 | 20.0 | 17.0 | 16.67 | – | – | – | – |
| 40GB50/50 | 12.0 | 15.0 | 25.67 | 25.67 | 8.5 | 11.0 | 14.67 | 18.0 |
| 60GP | 17.5 | 22.6 | 15.67 | 15.67 | – | – | – | – |
| 60GB50/50 | 12.0 | 16.0 | 26.67 | 27.33 | 11.0 | 15.0 | 17.67 | 17.67 |
| 80GP | 24.0 | 33.0 | 17.0 | 17.0 | – | – | – | – |
| 80GB50/50 | 13.2 | 19.0 | 26.0 | 28.0 | 11.5 | 15.5 | 21.0 | 21.0 |
| 100GP | 22.6 | 32.2 | 20.0 | 18.0 | – | – | – | – |
| 100GB70/30 | 20.0 | 29.0 | 25.67 | 25.67 | – | – | – | – |
| 100GB50/50 | 17.3 | 25.0 | 24.0 | 25.33 | 15.3 | 21.5 | 23.33 | 23.33 |
| 100GB45/45SF10 | 19.2 | 26.5 | 21.33 | 25.33 | – | 25.0 | – | 21.33 |
| 100GB30/70 | 11.8 | 16.9 | 25.67 | 28.33 | 8.9 | 13.0 | 22.0 | 22.0 |

recorded both on the perpendicular and diagonal arms, preceding and following formwork removal.

It should be noted, the differences in temperature between the center and the surface of the columns were highest along the diagonal arm, Arm (45), followed by the middle, Arm (60), and perpendicular, Arm (90), arms. This was anticipated considering the rate of heat loss at the corner of the cross-section was highest due to a larger surface area being available from which heat could be dissipated.

Results indicate that at the 50% slag replacement level, the maximum temperature difference realized by the 40-, 60- and 80-MPa columns was below 20°C. In contrast to this, the maximum temperature differences recorded by the GP columns at the same strength grades exceeded 20°C, peaking at 33°C for the 80-MPa column compared with 19°C for its companion 80GB50/50.

At the 100-MPa strength level, only the column incorporating 70% slag within the binder successfully maintained a maximum temperature difference below 20°C attaining a maximum of 16.9°C. The column containing 50% slag recorded a maximum temperature difference of 25°C. A direct comparison can be made of this column with the triple blend incorporating 10% silica fume. Incorporating silica fume into the binder resulted in an increased temperature difference, the triple blend attaining a maximum difference of 26.5°C. Once again, however, the largest temperature difference was realized by the GP column, recording a 32.2°C difference in surface to center temperature.

### 4.2. Temperature distribution

As expected, high in situ temperatures were developed in the core of the concrete columns which gradually subsided towards the column surface. The temperature variation encountered within the column cross-sections was found to be highly non-linear. The non-linear temperature distributions resulted in the rate of change of temperature with distance becoming very high near the surface of the columns.

### 4.3. Thermal gradients

The largest difference in temperature between the center and surface of the columns occurs along Arm (45). Despite this, the largest thermal gradient was encountered along Arm (90), implying that the rate of change of temperature with distance on this arm was the highest, despite the absolute temperature difference between the center and surface being the lowest. This trend was evident in all the columns investigated with the exception of the 100GB50/50 columns as shown in Table 5. The thermal gradients were found to be the highest at or near the column face.

### 4.4. The effect of concrete strength grade

Table 5 shows that the maximum thermal gradients generally increased with increasing concrete strength grade. The 40-, 60-, 80- and 100-MPa columns incorporating 50% slag into the binder recorded thermal gradients of 52, 60, 72 and 86°C/m, respectively. A similar trend was observed by the GP columns recording thermal gradients of 76, 108, 136 and 128°C/m at the 40-, 60-, 80- and 100-MPa strength grades. It should be noted that for the GP columns, a slight drop in thermal gradients was obtained by the 100-MPa column.

A similar trend was observed by Cook et al. [3] who investigated the development of thermal stresses in $1000 \times 1000$ mm columns of 35-, 90- and 120-MPa strength. They found that the lowest thermal gradient was obtained by the 120-MPa column while the 35- and 90-MPa columns produced approximately equal thermal gradients.

### 4.5. The effect of slag content

At all the strength grades investigated, incorporating slag into the binder substantially reduced the thermal gradients developed as shown in Table 5. In fact, at 50% slag replacement, the amount of benefit derived by incorporating slag into the binder increased with increasing strength grade up to the 80-MPa level. At the 40-, 60- and 80-MPa strength

Table 5
Thermal gradients at the time of peak temperature

| | Thermal gradients at the time of peak temperature (°C/m) | | |
|---|---|---|---|
| Column designation | Arm (90) | Arm (60) | Arm (45) |
| 40GP | 76 | 66.9 | 56.6 |
| 40GB50/50 | 52 | 41.5 | 34 |
| 60GP | 108 | 105.6 | 62.3 |
| 60GB50/50 | 60 | 51.9 | 55.8 |
| 80GP | 136 | 112.7 | 98.9 |
| 80GB50/50 | 72 | 59.9 | 55.2 |
| 100GP | 128 | 1197 | 103.7 |
| 100GB70/30 | 109 | 103.8 | 69.7 |
| 100GB50/50 | 86 | 90.1 | 94.9 |
| 100GB30/70 | 64 | 70.6 | 48.7 |
| 100GB45/45SF10 | 91 | 80.9 | 65.8 |

grades a reduction in thermal gradient along Arm (90) of 31%, 44% and 47%, respectively, was recorded in comparison to the GP columns. At the 100-MPa level, the reduction was a modest 32%.

Furthermore, at the 100-MPa level, the thermal gradients encountered were substantially alleviated with increasing slag content. At 0%, 30%, 50% and 70% slag replacement thermal gradients of 128, 109, 86 and 64°C/m were recorded. The smallest thermal gradient of 64°C/m recorded by the 100GB30/70 column was exactly half of the 100GP column. Maximum thermal gradients in excess of 100°C/m were obtained by all the GP columns at all the strength grades investigated with the exception of the 40GP column which developed a maximum thermal gradient of 76°C/m. In comparison, all the slag blends at all the strength levels evaluated, containing 50% slag or greater, developed thermal gradients below 100°C/m.

## 5. Conclusions

(1) The peak and net temperature rise encountered at the center of the columns are substantially reduced with the inclusion of slag into the binder. A progressive reduction in maximum net temperature rise is obtained with increasing slag content.

(2) The inclusion of slag into the concrete binder results in a delay in the time required to attain peak temperature in comparison to the GP concrete, irrespective of strength grade.

(3) Incorporating slag into the concrete mitigated the difference in temperature between the center and surface of the columns. The optimum benefit of utilising slag is derived if formwork removal is delayed from 24 to 48 or 72 h.

(4) Removal of the formwork at 24 h exacerbated the temperature difference between the center and surface of the columns containing a slag replacement equal to or greater than 50%. Despite this, the slag blends outperformed the GP columns with respect to alleviating temperature differentials.

(5) At 50% slag replacement, the maximum temperature difference recorded by the 40-, 60- and 80-MPa columns was below 20°C, while temperature differences recorded by the GP columns at the same strength grades exceeded 20°C.

(6) Thermal gradients increased with increasing concrete strength grade. The maximum thermal gradients exhibited by the GP columns were significantly reduced when slag was incorporated into the concrete.

## Acknowledgments

The project was funded by Independent Cement and Lime and Blue Circle Southern Cement. The authors acknowledge the companies' financial support and their commitment to research and development. The authors are especially grateful to Mr Alan Dow and Mr. Tom Wauer from Independent Cement and Lime and Dr. Ihor Hinczak of Blue Circle Southern Cement.

## References

[1] Y.S. Hwee, B.V. Rangan, Studies on commercial high strength concrete, ACI Mater J 87 (1990) 440–445.
[2] N.A. Lloyd, B.V. Rangan, High strength concrete: a review, Research Report No. 1/93, 1993, School of Civil Engineering, Curtin University of Technology, Perth, WA.
[3] D. Cook, M. Buquan, P.-C. Aitcin, D. Mitchell, Thermal stresses in large high-strength concrete columns, ACI Mater J 89 (1) (1992) 61–68 (Jan.–Feb.).
[4] P.-C. Aitcin, P. Laplante, C. Bedard, Development and experimental use of a 90 MPa (13,000 Psi) field concrete, High Strength Concr SP-87 (1985) 51–70 (CI, Detroit).
[5] R.L. Yuan, M. Ragab, R.E. Hill, J.E. Cook, Evaluation of core strength in high strength concrete, Concr Int 13 (5) (1991) 30–34 (May).
[6] B. Sioulas, J.G. Sanjayan, The effect of slag blended cements on the in-situ strength of high strength concrete columns, Concrete 95 Toward Better Concrete Structures, Proceedings CIA Conference, 4–7 Sept., Concrete Institute of Australia, Brisbane, 1995, pp. 531–539.
[7] K. Koibuchi, H. Yamaguchi, K. Kabota, Y. Ishikawa, Hydration and compressive strength development of high strength concrete heated to 60 or 80°C at the early age, Proceedings of Cement and Concrete, No. 45, Concrete Association of Japan, 1991, pp. 204–209.
[8] S.J. Thurston, N. Priestly, N. Cooke, Thermal analysis of thick concrete sections, ACI J Proc 72 (38) (1980) 347–357.
[9] J.G. Sanjayan, Control of thermal cracking in high strength concrete using a slag blended cement, Concr Aust 21 (1) (1995) 10–13 (April).
[10] S. Sarkar, P.-C. Aitcin, H. Djellouli, Synergistic roles of slag and silica fume in very high strength concrete, Cem Concr Aggregates 12 (1) (1990) 32–37.
[11] R.W. Carlson, D.L. Houghton, M. Polivka, Causes and control of cracking in unreinforced mass concrete, ACI J Proc 76 (7) (1979) 821–837 (July).
[12] ACI Committee 207, Effect of restraint, volume change and reinforcement on cracking of massive concrete, ACI J Proc 70 (45) (1973) 445–470 (July).
[13] S.L. Mak, Factors influencing the in-situ strength in high strength concrete columns, Thesis submitted in fulfillment of the requirements for the degree of Doctor of Philosophy, Department Civil Engineering, Monash University, Australia, 1993.
[14] S. Smeplass, M. Maage, Heat of hydration of high strength concretes, Proceedings 2nd International Symposium on Utilization of High Strength Concrete, University of California, Berkeley, American Concrete Institute, Detroit, Michigan, 1990, pp. 31 (May).
[15] S.L. Mak, A. Lu, Engineering properties of high performance concretes containing blast furnace slag under in-situ moisture and temperature conditions, Proceedings of ACI International Conference on High Performance Concrete, Singapore, American Concrete Institute, Detroit, Michigan, 1994, pp. 159–175 (Nov.).
[16] P.J. Wainright, J.J.A. Tolloczko, Early and later age properties of blast furnace slag cements, mortars and concrete, ACI J 79 (1982) 444–457 (Nov.–Dec.).
[17] K. Kokubu, S. Takahashi, H. Anzai, Effect of curing temperature on the hydration and adiabatic temperature characteristics of Portland Cement — blast furnace slag concrete, in: V.M. Malhotra (Ed.), ACI SP-114, American Concrete Institute, Detroit, Michigan, 1989, pp. 1361–1375.
[18] M. Yurugi, T. Mizobuchi, T. Teruachi, Utilization of blast-furnace slag and silica fume for controlling temperature rise in high strength concrete, ACI SP-132, 1992, pp. 1433–1450.
[19] F. Collins, W. Green, Testing and modeling to assess early age thermal cracking risk, Concr Aust CIA 20 (4) (1994) 17–20.